

IMPROVING PUSH BELT CVT EFFICIENCY BY CLAMPING FORCE CONTROL STRATEGIES BASED ON VARIATOR SLIP MEASUREMENT

Maaïke van der LAAN and Mark van DROGEN

Van Doorne's Transmissie b.v. / Bosch Group, P.O.Box 500, 5000 AM, Tilburg, The Netherlands

Developments in clamping force control for the push belt Continuously Variable Transmission (CVT) aim at increased efficiency in combination with improved robustness. Current control strategies attempt to prevent macro slip between elements and pulleys at all times for maximum robustness.

In order to search for the limiting factors in developing a new control strategy, situations where macro slip occurs have been investigated. An important failure mechanism proves to be the occurrence of adhesive wear in the contact leading to a loss in torque transfer. As a combination of normal load and slip speed, respectively clamping force and slip rate in a variator, a transition can be found from a safe wear region to an excessive/adhesive wear region. The occurrence of this transition has been verified with experiments on CVT variator level. It turns out that macro slip is acceptable to a certain extent.

The new wear insight allows fundamental different control strategies. In particular strategies based on CVT slip measurement and control are of interest. These control strategies enable lower clamping forces while retaining robustness. Consequently, CVT efficiency increases which will lead to an improvement in fuel consumption of approximately 5%.

Keywords: Push Belt CVT, Variator Robustness, Fuel Economy, Macro Slip, Slip Control, Tribology

1. INTRODUCTION

The market for belt type Continuously Variable Transmissions (CVTs) is rapidly growing. Since belt production start up at Van Doorne's Transmissie (VDT) in 1985, more than 5 million vehicles have been equipped with a push belt CVT. At this moment, 1.2 million push belt CVTs per year are used in the Japanese, North American, European, Korean and Chinese markets. About 50 different vehicle models are currently available with push belt CVT. Figure 1.1 shows the Van Doorne push belt, Figure 1.2 illustrates the working principle of the push belt variator.

To further extend the application range of its push belt, VDT is examining more severe requirements regarding transmittable power, transmission size (centre distance), ratio coverage and durability. To meet those requirements, the power density of belt and pulley needs to be increased (1). The current push belt status is nicely shown by the Nissan Murano with push belt CVT that has a ratio coverage of 5.4 and can cope with a 3.5 liter V6 180 kW/350 Nm engine with torque converter, applying drive side torque levels on the belt that lie above 500 Nm (2).

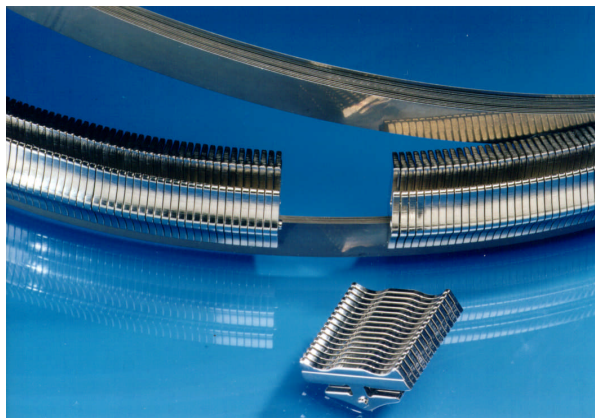


Figure 1.1 Example of a partly disassembled Van Doorne push belt with approximately 400 elements and 2 sets of 9 rings.

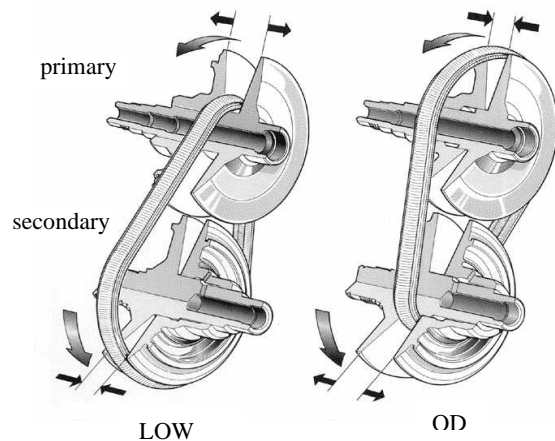


Figure 1.2 Example of a push belt variator and its working principle. In the variator, power is transmitted from the primary to the secondary pulley by means of friction between the push belt elements and the pulley sheaves. Stepless shifting between the extreme ratios LOW and OverDrive (OD) is realised by changing the axial position of the moveable pulley sheaves through changing the pulley clamping forces.

Besides increasing power density, VDT developments aim at improving the vehicle fuel consumption by improving CVT-efficiency (3). Figure 1.3 shows the fuel consumption of manual transmissions (MTs) compared to their CVT counterpart. Among these the recently introduced Mercedes-Benz A-class CVT, applicable for engine torque levels up to 280 Nm with a ratio coverage of 6.4 (4). For these applications, the fuel consumption of the CVT is comparable to the MT level. In general, possibilities for further improvement of the fuel consumption of state-of-the-art-CVTs are: increasing the ratio coverage, reducing actuation losses and decreasing variator clamping forces, for instance by application of torque fuse (3). In (3) it is shown that a decrease in variator clamping forces (compared to the state-of-the-art control strategy) can lead to a decrease in fuel consumption of 5%. The investigation presented in this paper is aimed at realising this.

Lowering the variator clamping forces is beneficial for both fuel consumption, because of the decrease in power consumed by the CVT hydraulic pump, and power density, because of the decrease in push belt stresses. By lowering the clamping forces, the risk of belt slip increases, for instance in case of torque peaks, or slow or delayed hydraulic responses. One of the consequences of excessive belt slip can be severe wear in the element/pulley contact.

For future improvements of the clamping force control strategy it is important to determine the failure limits for the variator system. The results of this investigation are described in this paper.

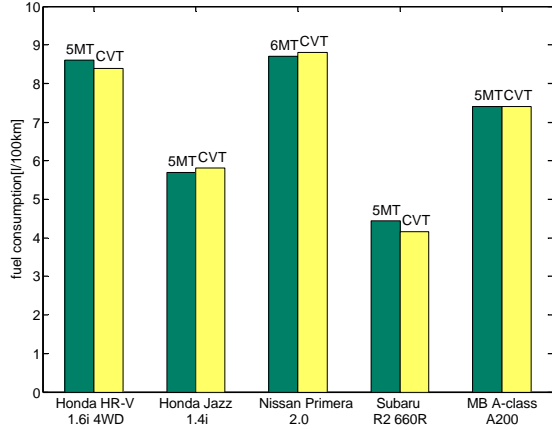


Figure 1.3 Comparison Manual Transmission (MT) versus CVT for a drive cycle. Source: vehicle documentation.

In Chapter 2 macro slip and the variator failure mode are discussed. In Chapter 3 the measurement results of determining the variator failure diagram are presented. Chapter 4 discusses the consequences of the measurement results for future variator control strategies. Finally the conclusions of this investigation are summarised.

2. MACRO SLIP AND VARIATOR FAILURE MODE

Micro and macro slip are defined and explained in Section 2.1. Section 2.2 describes the variator failure mode. In Section 2.3 wear and failure diagrams are described.

2.1 Belt-Pulley Micro/Macro Slip

In the push belt CVT system, torque is transmitted by means of friction between the belt elements and the pulley sheaves. Therefore, the maximum transmittable torque is determined by the normal force and the coefficient of friction. This situation can be explained by means of a so-called slip curve (5) as is shown in Figure 2.1.

On the horizontal axis of the slip curve, the primary or input torque T_p is denoted and on the vertical axis the slip rate. The slip rate s_r (%) is defined as

$$s_r = \frac{i_s - i_0}{i_0} \cdot 100\% \quad (1)$$

where the speed ratio $i_s = n_p/n_s$ and i_0 equals the initial i_s at the no-load condition (spin loss). At the variator test rig the secondary or output torque T_s will be adjusted and the input torque T_p is automatically adjusted by keeping the primary rotational speed at a constant value. It is customary at VDT that T_p is labelled instead of T_s .

As can be seen in Figure 2.1, higher torque levels will result in an increase in slip rate which is indicative of the slip speed between belt elements and pulley sheaves. The maximum transmittable torque $T_{p,max}$ is reached when all elements in the pulley with the lowest clamping force are needed for torque transfer. Higher torques cannot be transmitted and the result is a sharp increase in the slip rate and the slip speed between belt elements and pulley sheaves.

The slip rate is defined as micro slip when the slip rate level is below the slip rate level at $T = T_{p,max}$. Along the same lines, macro slip is defined as the slip rate when the slip rate level is above the slip rate level at $T = T_{p,max}$, as shown in Figure 2.1.

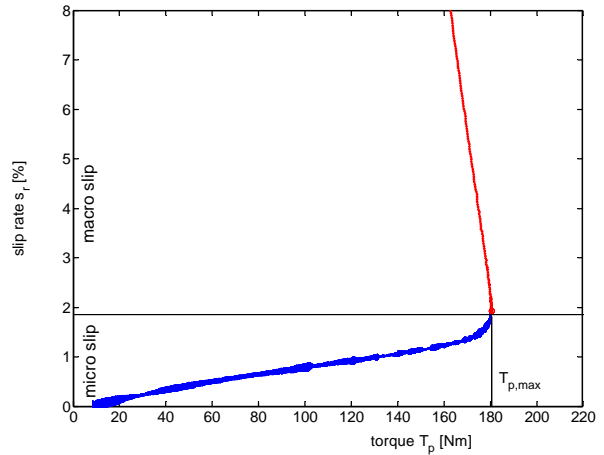


Figure 2.1 Slip curve measurement in TOP ratio.

In the macro slip regime it is possible to determine the coefficient of friction μ in the contact between belt element and pulley sheave based on the measured torque. In the macro slip regime, all elements are transferring torque and are slipping. Hence the kinetic coefficient of friction μ can be determined by

$$m = \frac{T_p \cos \lambda}{2r_p F_{ax,s}} \quad (2)$$

where T_p is the primary torque, λ is the cone angle and r_p represents the primary running radius. The coefficient of friction at $T_{p,max}$ is used to characterise the torque capacity of the system (5).

2.2 Belt-Pulley Failure Mode

A belt-pulley failure mode investigation presented in (6) shows that excessive slip may lead to excessive wear in the contact between element and pulley. This may result in reduced torque capacity and/or modified element and pulley geometry. From this investigation, it is concluded that the occurrence of severe, adhesive wear in a slip event must be prevented and that the transition from mild to severe, adhesive wear must be regarded as a failure mode. Furthermore, it became clear that this transition does not have to coincide with the transition from micro to macro slip, which is quite often erroneously assumed.

In the next section, a more fundamental approach to wear and transitions/failure is taken in order to understand the phenomena described above.

2.3. Wear and Failure Diagrams

2.3.1. Wear Theory

In general it is possible to distinguish several mechanisms that lead to wear of an engineering component in a lubricated contact. These wear mechanisms are:

1. tribochemical wear
2. abrasive wear
3. fatigue
4. adhesive wear

For the investigation of the slip failure mode of the variator, attention is focussed on adhesive wear. At the moment the consensus is that the transition from a relatively mild wear region (governed by mechanisms 1, 2 and 3) to severe wear (mechanism 4: adhesive) must be prevented at all times. Very short slip events in the adhesive wear region will cause a deterioration of the torque capacity whereas experience shows that the torque capacity does not change under the assumed safe operating conditions in the micro slip regime. Diagrams dealing with the transitions in wear regimes and especially diagrams that cover the transition from mild to severe wear are described in the next section.

2.3.2 Failure Diagrams

The Stribeck curve usually maps (lubrication) regimes by means of the coefficient of friction as a function of operating conditions under mild wear conditions. To map failure modes (e.g. transition to adhesive wear) as a function of operating conditions, another diagram is needed. In literature these are known as transition, wear or failure diagrams. For more information the reader is referred to (6).

In this paper, the IRG-OECD transition diagram (7) will be adopted. Failure is mapped with regard to normal force F_N and sliding velocity v and therefore this diagram is also called the F/v-failure diagram. This corresponds closely to the variator situation: clamping force and slip. The F/v-failure diagram distinguishes between regions of efficient (mild wear) and inefficient (adhesive wear) performance in non-conforming lubricated sliding contacts. The failure criterion used is based on the change of friction level in a certain lubricated concentrated contact

For the element-pulley contact this is a useful criterion (cf. Figures 2.2, 2.3 and 3.2), whereas criteria only based on direct wear measurements (e.g. wear volume and/or wear rate k values) are difficult to derive because of the complex nature of the contacting bodies especially the geometry of the element flank, and in-situ wear evaluation is even more difficult to perform.

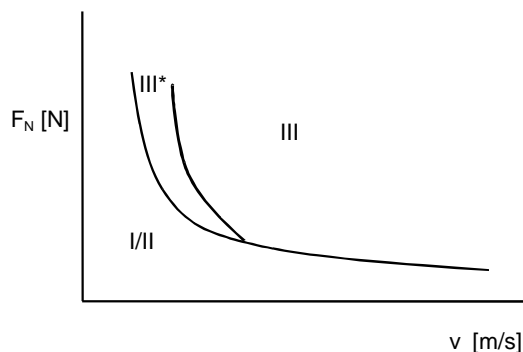


Figure 2.2 Transition diagram or F/v-failure diagram (reproduced from (7)).

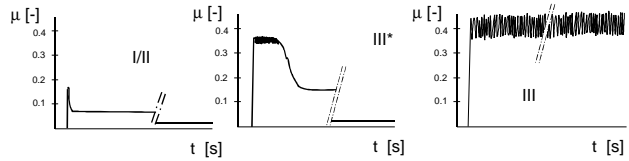


Figure 2.3 Coefficient of friction-time curves (7).

An example of the F/v-failure diagram is shown in Figure 2.2. In this diagram, where the so-called load-carrying capacity F_N is presented as a function of the sliding velocity v , three regions, separated by two transition curves, can be distinguished. These regions are governed by the measured friction time characteristics seen in Figure 2.3.

Region I/II is considered to be a mild wear or 'safe' region, where friction is relatively low ($\mu = 0.15$ or less) and wear is virtually negligible (wear rate $k \approx 10^{-8} \text{ mm}^3/\text{Nm}$). The lubricating conditions in this region are boundary lubrication (BL), mixed lubrication (ML) and elasto-hydrodynamic lubrication (EHL). In region III* there is incipient scuffing: material transfer takes place at a microscopic scale and the average contact pressure (p_{av}) decreases. In this region, initial values of $\mu \approx 0.35$ and $k \approx 5 \cdot 10^{-6} \text{ mm}^3/\text{Nm}$ occur, both decreasing with time. If the contact is to operate in region III, it fails almost immediately by scuffing, with $\mu \approx 0.4$ and $k \approx 10^{-3} \text{ mm}^3/\text{Nm}$. In this region very severe adhesive wear (material transfer) will take place.

In the next chapters the F/v-failure diagram for the variator is determined based on measurements.

3. DETERMINATION OF VARIATOR F/V-FAILURE DIAGRAM

Figure 3.1 shows a schematic view of the test rig used. To determine the variator F/v-failure diagram, it is necessary to be able to calculate the slip speed and normal force levels in the contact of belt element and pulley sheave. A method is described in (6). Furthermore, a procedure is needed to control the variator slip speed and normal force in a predetermined manner. This procedure is also presented in (6).

3.1 Determination of the Adhesive Wear Limit

Similar to the theory described in Section 2.3.2, the adhesive wear transition is primarily detected by looking at the torque signals (or coefficient of friction) over the course of time. Since the clamping force levels are chosen to be approximately constant during the test, a sudden increase in torque is associated with increased torque transmittance/friction caused by adhesive wear. This is especially clear when looking at the calculated coefficient of friction during the test.

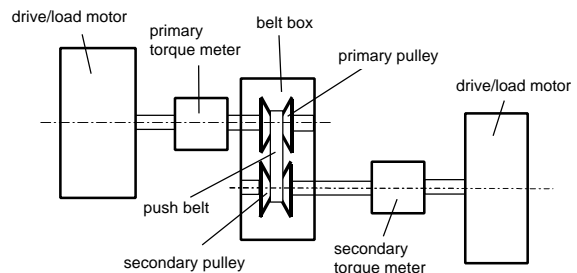


Figure 3.1 Schematic view of the test rig

Figure 3.2 shows the torque signal and calculated coefficient of friction during two different tests. The top shows the torque, slip speed and coefficient of friction for a slip event in OD that did not cause adhesive wear. The bottom shows the same signals for a measurement that did cause adhesive wear. The arrow indicates the start of the adhesive wear. The measurements are from the same belt and were performed right after each other. For the second measurement the maximum slip speed level was increased as compared to the first one (8.3 vs. 9.7 m/s).

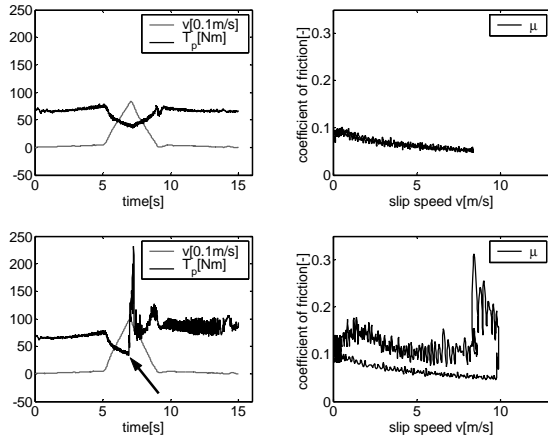


Figure 3.2 Above, the torque, slip speed and coefficient of friction for a slip event in OD that did not cause adhesive wear. Below, the same signals for a measurement that did cause adhesive wear.

3.2 The Variator F/v-Failure Diagram

For each parameter setting the slip speed at the point of failure was determined (the slip speed corresponding to the arrow in Figure 3.2) and displayed in an F/v-failure diagram.

Figure 3.3 shows the variator failure diagram for a selection of measurements:

- all at a primary speed of 1500 rpm except test no.5, which was at a primary speed of 2200 rpm,
- in two different ratios (LOW and OD),
- and at different normal force levels.

For test no.5 a higher failure limit than the indicated slip speed is valid, because the belt did not fail at this slip speed, but the slip speed could not be increased because the secondary pulley speed had reached zero.

Note that the F/v-failure diagrams presented in this paper are valid for the used hardware, lubrication fluid type and running-in procedure.

The influence of variator ratio and clamping force level can be summarised as follows: the influence of the variator ratio: when the measurements at the same element normal force level and in different ratios are compared (LOW vs. OD), the LOW measurement always fails earlier in terms of slip speed level compared to OD.

The influence of the clamping force level: as is expected based on theory (see Section 2.3.2) the higher the normal force the smaller the failure limit slip speed. See (6) for a comparison of the F/v-failure diagram that resulted from the variator measurements with that from literature. In the next chapter the consequences of the F/v-diagram investigation for the clamping force control strategy will be discussed.

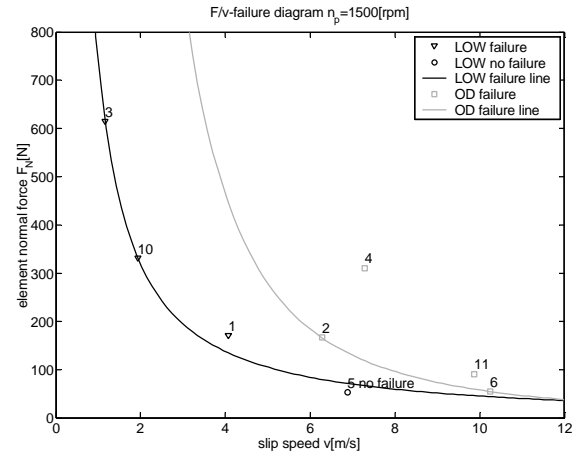


Figure 3.3 F/v-failure diagram measured at a primary speed of 1500 rpm.

4. CONTROL STRATEGY DISCUSSION

The current control strategy is described in Section 4.1. Section 4.2 discusses control strategy improvements based on the F/v-failure diagram.

4.1 Current Control Strategy

Figure 4.1 shows the controlled safety as a function of the actual primary torque relative to the maximum engine torque. A conclusion is that low torque levels correspond to high safety levels. Especially stationary, part load conditions (driving constant speed) lead to high overclamping in order to prevent macro slip.

The high safety in part load causes a drawback on efficiency. Figure 4.2 shows an example of measured variator efficiency in LOW and OD. Slip losses increase and the torque losses decrease with decreasing safety.

Therefore the variator efficiency shows an optimum. For LOW this optimum is reached at a safety around 1.3, for OD this optimum is reached for a safety around 1.1. The extra loss in the variator in part load caused by the high safety strategy is around 2% in OD at safety 2 and more than 6% at safety 4 and higher. In LOW the extra loss is around 1% at safety 2 and more than 4% at safety 4 and higher.

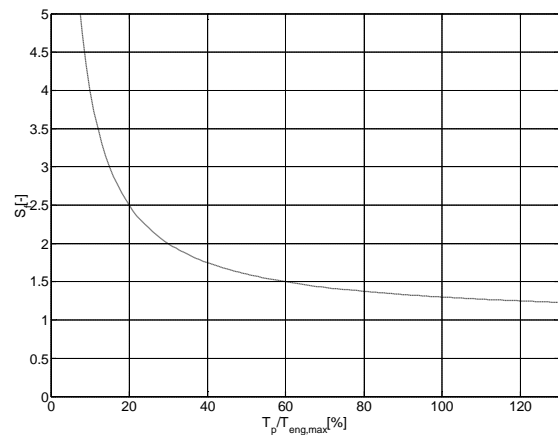


Figure 4.1 Controlled safety with the current control strategy as a function of primary torque relative to maximum engine torque.

When besides the losses in the variator, the other losses in the CVT are also considered the extra loss in efficiency will be even more, because actuation losses also decrease with decreasing safety. This implies that the safety corresponding to optimal CVT efficiency is lower than 1.3 in LOW and lower than 1.1 in OD.

In (3) it is shown that the increase in variator clamping forces of the current control strategy compared to the clamping force levels corresponding to safety 1.3 leads to an increase in fuel consumption over the NEDC cycle of more than of 5%.

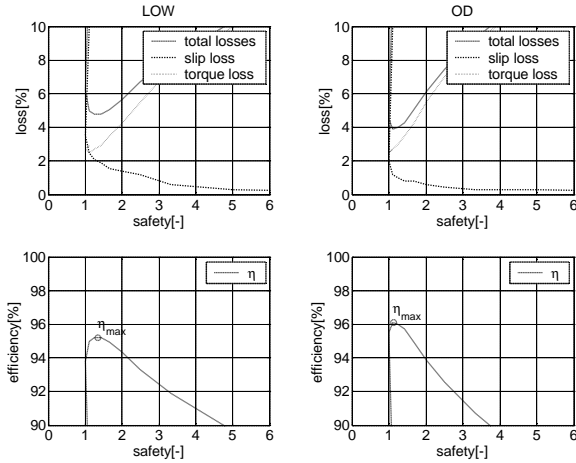


Figure 4.2 Variator losses and efficiency as a function of safety in LOW and OD.

4.2 Control Strategy Improvements Based on the F/v-Failure Diagram

By determining the origin of adhesive wear, and displaying the failure lines in the F/v-failure diagram, it is possible to change the basics of the clamping force control strategy from preventing macro slip at all times to allowing limited macro slip but preventing crossing the failure lines in the F/v-failure diagram. This will result in a decrease in overclamping and therefore an increase in efficiency.

4.2.1 Control Strategy Options

As already stated in the introduction, it is possible to change the basics of the clamping force control strategy from preventing macro slip at all times to allowing limited macro slip but preventing crossing the failure lines in the F/v-failure diagram.

There are several relative simple possibilities to realise this. One is to limit pulley clamping force $F_{ax,s}$ based on a measured or even a maximum possible slip speed v . For instance in LOW with positive torque, the maximum slip speed is reached when the secondary pulley speed is reduced to zero. For the P811 variator (see Table 2.1) for a primary pulley speed of 1000 rpm in LOW, the slip speed cannot be higher than about 3.1 m/s. The clamping force can be controlled to a maximum limit in this case in order to avoid crossing the failure lines in the failure diagram.

Other way around, it is also possible to limit the slip speed v depending on the applied clamping force $F_{ax,s}$. This can be realised by limiting the controlled speed ratio or primary rotational speed.

In (8) a control strategy based on adaptation of the clamping force is discussed. Another way to realise optimal efficiency while avoiding adhesive wear is CVT slip control: clamping force control based on a measured slip signal instead of estimated torque levels. Figure 4.3 shows a control scheme of the current control strategy compared to CVT slip control.

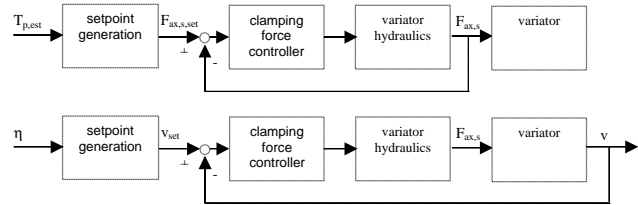


Figure 4.3 The current control strategy (above) versus CVT slip control (below).

For the current control strategy, measurement of $F_{ax,s}$ is necessary, so this requires secondary pressure measurement. For slip control instead of secondary pressure measurement, measurement of variator slip is necessary. To determine v , both rotational speeds (ω_p and ω_s) and geometrical ratio i_0 need to be determined. Measurement of the geometrical ratio can be realised by measuring one of the running radii of the variator or the position of one of the moveable pulley sheaves. When the variator is against the LOW or OD stop, the geometrical ratio is also known.

By directly controlling the desired slip level it is possible to control the optimum efficiency in stationary situations. This point of optimum efficiency will always be in the micro slip regime. Controlling macro slip in stationary situations (constant vehicle speed) is not desired because of the fact that the optimum efficiency is reached under micro slip conditions. Figure 4.2 shows that with increasing slip CVT efficiency decreases sharply.

A torque disturbance at the wheels of the vehicle will lead to a disturbance in the measured slip. Short time macro slip is no problem as long as the controller guarantees that the failure limits in the F/v-diagram are not reached. From the F/v-failure diagram the necessary control accuracy in case of disturbances that cause short time macro slip can be derived. The position of the failure lines in the F/v-diagram will serve as a basis for the specification for the requirements the clamping force control system (delay, clamping force increase/decrease rate).

An example of a slip controller design applied in a vehicle is presented in (9) and (10). The next section shows an example of slip control applied at a test rig.

4.2.2 Slip Control Example in the F/v-failure Diagram

Figure 4.4 shows an example of slip control at a test rig. The test rig controls take care that the primary speed is controlled at a constant level. The secondary torque is controlled in such a way that the primary torque is 62 Nm with a torque peak up to 102 Nm at $t=5$ s. The variator is against the stop in geometrical ratio OD. The slip rate is measured and controlled by a simple PI-control algorithm. The aim is to control a constant slip rate of 1%. During the steady state situation, this slip level is accurately controlled. The torque peak causes a short macro slip peak of about 6%, the slip controller increases the clamping force which causes the slip to reduce. After the peak, the clamping force is reduced slowly to control the setpoint of 1% slip.

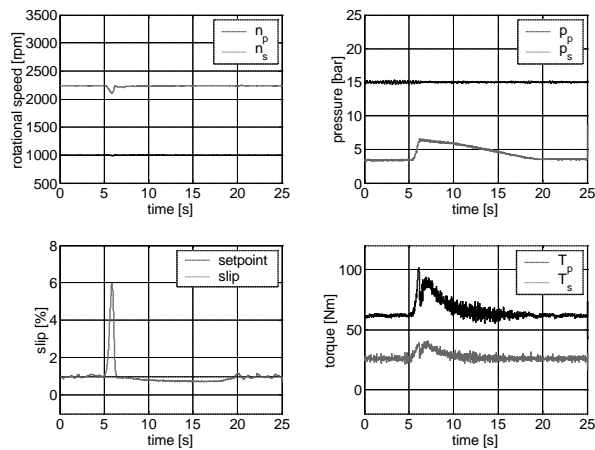


Figure 4.4 Variator slip control example.

Figure 4.5 shows the same measurement in the F/v-diagram. The clamping force/slip speed combination is far from the failure line, so there is no risk of adhesive wear and also no adhesive wear was observed.

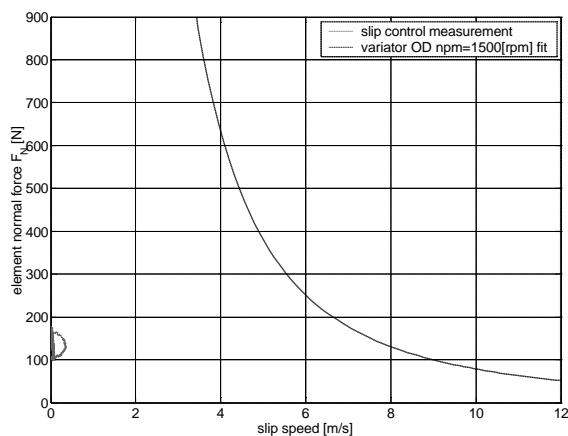


Figure 4.5 Trajectory of the variator control strategy example of Figure 4.4 in the F/v-failure diagram.

5. CONCLUSION

The main conclusion of this paper is that the presented F/v-failure diagram can be used to optimise the variator control strategy by applying lower clamping forces in order to realise improved fuel consumption (of approximately 5%) and power density without compromising robustness for adhesive wear.

Furthermore it can be concluded that:

- The occurrence of adhesive wear leads to a decrease in variator torque capacity and must therefore be regarded as a variator failure mode.
- Adhesive wear in the belt/pulley contact is caused by a combination of a too high slip speed and clamping force level.
- With respect to adhesive wear, macro slip is acceptable to a certain extent. The allowed macro slip rate depends on the operating conditions.
- A first estimation of the failure limit for the variator is determined by measurements and displayed by a failure line in the F/v-failure diagram.

- In general the relation between normal force and slip speed that describes the adhesive wear failure limit of the variator is similar to the theory.
- Besides slip speed and clamping force, the measurements show that the occurrence of wear also depends on the geometrical ratio (LOW more critical than OD) and the primary speed (the lower the more critical).
- New possible control strategies are based on CVT slip measurement and control.
- Control strategy application examples show that it is possible to change the basics of the clamping force control strategy from preventing macro slip at all times to allowing limited macro slip but preventing crossing the failure lines in the F/v-failure diagram.

6. REFERENCES

- (1) Brandsma, A., Lith, J. van, Hendriks, E., Push belt CVT developments for high power applications, Proc. of CVT99, Eindhoven University of Technology, (1999)142-147.
- (2) Sluis, F. van der, Brandsma, A., Lith, J. van, van der Meer, K., Velde, A. van der, Pennings, B., Stress reduction in push belt rings using residual stresses, Proc. of CVT2002 Congress, VDI-Berichte 1709, Munich, (2002)383-402.
- (3) Spijk, G. van, Veenhuizen, P.A., "An upshift in CVT-efficiency", Proc. of Getriebe in Fahrzeugen '98. VDI-Berichte 1393, Friedrichshafen, (1998)659-671.
- (4) Greiner, J., Kiesel, J., Lorch, Veil, A., Strenkert, J., Front-CVT Automatikgetriebe (WFC280) von Mercedes-Benz, New front wheel drive CVT (WFC280) from Mercedes Benz., Proc. of Getriebe in Fahrzeugen '04. VDI-Berichte 1827, Friedrichshafen, (2004)421-445.
- (5) Pennings, B., Drogen, M. van, Brandsma, A., Ginkel, E. van, Lemmens, M., Van Doorne CVT Fluid Test – A Test Method on Belt-Pulley Level to Select Fluids for Push Belt CVT Application, SAE 2003-01-3253, Proc. of the 2003 Powertrain & Fluid Systems Conference, Pittsburgh, (2003).
- (6) Drogen, M. van and Laan, M. van der, Determination of Variator Robustness under Macro Slip Conditions for a Pushbelt CVT, SAE 2004-01-0480, SAE 2004 World Congress, Detroit, (2004).
- (7) Schipper, D.J. and Gee, A.W.J. de, Lubrication Modes and the IRG Transition Diagram, Lubrication Science 8-1, (1995)27-35.
- (8) Laan, M. van der and Drogen, M. van, Brandsma, A., Improving Push Belt CVT Efficiency by Control Strategies Based on New Variator Wear Insight, CVT 2004 Congress, San Francisco, (2004).
- (9) Bonsen, B., Klaassen, T.W.G.L., Meerakker, K.G.O. van de, Steinbuch, M., Veenhuizen, P.A., Measurement and control of slip in a continuously variable transmission, IFAC Mechatronics 2004, Sydney, (2004).
- (10) Veenhuizen, P.A., Variator Slip Control Implemented in a Production Vehicle with Push Belt CVT, IIR/CTI Symposium, Würzburg, (2004).